JOURNAL OF MATERIALS SCIENCE. MATERIALS IN MEDICINE 5 (1994) 495–499

Layered, adhesively bonded hydroxyapatite coatings for orthopaedic implants

S. L. EVANS, K. R. LAWES, P. J. GREGSON
Engineering Materials, University of Southampton, Southampton SO9 5NH, UK

A method of producing layered, adhesively bonded hydroxyapatite coatings is described. The coatings have a flexible polymeric interlayer which can improve load transfer from the implant to the bone, and a hydroxyapatite-rich surface which can provide mechanical interlocking with the bone. The coatings have been characterized using a number of methods including optical and electron microscopy, mechanical testing and finite element analysis. Some ways in which the coatings could be used to produce orthopaedic implants with improved mechanical and biological compatibility are discussed.

1. Introduction

Hydroxyapatite coatings are increasingly widely used to promote the cementless fixation of orthopaedic implants by encouraging intimate bone apposition to the implant surface [1–4]. Layered, adhesively bounded hydroxyapatite coatings [5] have a number of possible advantages over conventional plasma-sprayed coatings, including an improvement in the fatigue strength of the substrate [6] and improvements in the mechanical compatibility of the prosthesis through the use of a layered structure with appropriate elastic properties [7]. In order to use such layered coatings effectively, a method of applying them to curved or textured surfaces of implants and of ensuring the exposure of hydroxyapatite at the surface is needed. The present paper describes such a method, together with the characterization of the resulting coatings.

2. Methods and materials

The coatings contained commercial hydroxyapatite powder ("Captal", Tate and Lyle), in 1 μm and 250 μm particles. The larger particles were roughly spherical clusters of sintered grains and were porous, allowing a high degree of mechanical interlocking with the surrounding adhesive. A single part, heat-cured, toughened epoxy adhesive (Permabond ESPP770) was used; the adhesive viscosity being adjusted with fine hydroxyapatite powder as a filler, and with Cab-o-Sil fumed silica as a thixotroping agent.

The coatings had two layers, which were applied separately. The first layer is regarded as an optional interlayer applied to improve the mechanical compatibility of the implant and to give optimum bonding to the substrate. This layer incorporated 3.5 wt % fumed silica to prevent slump during curing, and was approximately 250 μm thick. This was then partially cured by heating to 150 ± 3 °C for 45 min, resulting in a solid interlayer which was sufficiently robust to withstand the subsequent application of the outer coating.

After the samples had been allowed to cool to room temperature, a layer of adhesive approximately 200 μm thick and containing 35 wt % 1 μm hydroxyapatite filler was applied and 250 μm hydroxyapatite particles were sprayed over it at an angle to prevent accumulation of excess particles on the implant surface; such particles can take up the adhesive by capillary action. The coatings were then cured for 70 min at 150 ± 3 °C and allowed to cool. The coatings were then bead-blasted using 150 μm glass beads for 10 s or 60 s, at air pressures of 10, 30 and 50 psi. A control was prepared by milling with a single-point cutting tool at high speed, leaving a coating approximately 150 μm thick.

Representative areas were stained using 2% aqueous alizarin red S at pH 4.1, and observed using a Wild stereo-macroscope; a Kontron image analyser was then used to quantify the amount of exposed hydroxyapatite. Samples were vacuum impregnated with epoxy resin, sectioned using a low-speed diamond saw and polished using standard metallographic methods. These sections were etched in 1% HCl to emphasize the hydroxyapatite particles and examined using polarized light microscopy. Samples were etched for 120 h in 1% HCl to simulate the resorption of the hydroxyapatite and were then gold-coated and examined using a JEOL T300 scanning electron microscope (SEM), together with unetched controls.

Sample coatings were applied to miniature tensile test pieces, and strained and examined in the SEM in order to assess their resistance to cracking and spalling during deformation of the substrate. A representative area was selected at the beginning of the test; this area was identified and photographed at each strain increment in order to study the initiation and propagation of cracks in the coating.

A simple double cantilever beam test was used to evaluate the strength of bonding of the coatings to the substrate. Sample coatings were applied to Ti–6Al–4V strips; uncoated strips were then bonded to them using a high viscosity cyanoacrylate adhesive.

0957–4530

The two strips were then separated at one end by a screw, and the length of the resulting crack was measured using a travelling microscope. A number of measurements could thus be taken from each specimen. Plasma-sprayed coatings were also tested for comparison.

X-ray diffraction measurements were used to study the structure of the coatings in comparison to a control prepared by plasma spraying. Measurements were taken using copper K_α radiation, scanning from 12–90° 2θ in 0.02° steps, with a count time of 5 s per step. The results were compared with standard diffraction data; profile fitting was used on four peaks in the range 31–34° 2θ in order to obtain full-width half maximum height measurements for comparison of line-broadening effects in the different coatings.

A simple finite element model was used to represent the effect of the coatings on the stress distribution around the distal part of a hip prosthesis. Three models were formulated, representing an adhesively bonded coating with a 2 mm interlayer, a plasma-sprayed coating and an unimplanted femur. The plasma-sprayed coating was modelled using 806 six-noded triangular axisymmetric harmonic elements while the adhesively bonded coating and the unimplanted femur were represented by 798 and 16 eight-noded quadrilateral axisymmetric harmonic elements, respectively. The elastic properties assumed for the bone, titanium alloy substrate and epoxy coating are shown in Table I; all three materials were assumed to have linear, isotropic properties for simplicity. It should be noted that since the plasma-sprayed coating and the titanium alloy were assumed to have the same elastic properties the coating did not need to be represented by a separate layer of elements. An axial load of 5000 N and a bending moment of 150 Nm were applied to the femoral diaphysis, representing a peak load during walking. The models were formulated and solved using the LUSAS finite element system (FEA Ltd).

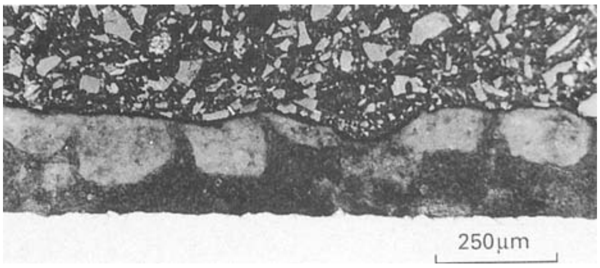

Figure 1 Optical micrograph showing a section through a typical coating with no interlayer after bead blasting.

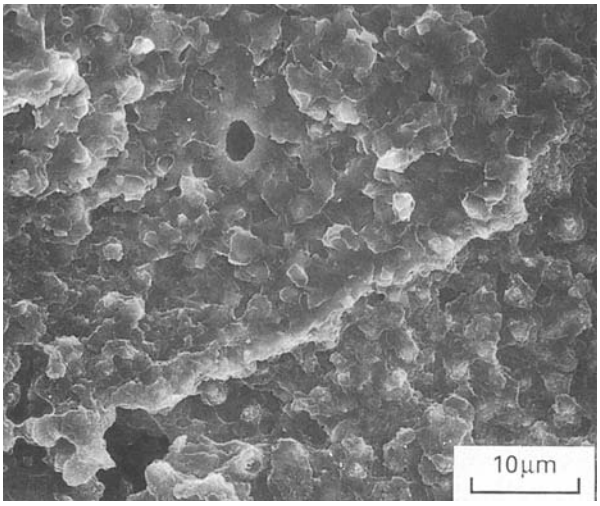

Figure 2 Scanning electron micrograph showing the interface between a particle and the surrounding adhesive. The picture shows the surface of a fracture normal to the plane of the coating.

3. Results

Fig. 1 shows a section of a typical coating; note that the interlayer was omitted in this specimen. The bonding process results in a closely packed base layer of particles which are well bonded to the substrate, but they are partially covered with adhesive and obscured by poorly bonded, superficial particles. Fig. 2 shows the interface between one of the particles in the base layer and the adhesive; the adhesive has penetrated deeply into the pores of the particle. During bead blasting, this adhesive penetration reinforces the most strongly bonded areas of the particles, so that superficial particles and the upper part of the base layer are quickly removed, but a strongly bonded layer of half-particles remains with a considerable area of exposed hydroxyapatite. The bead blasting process is therefore tolerant of variation in the blasting conditions, enabling its practical use for the production of coatings on uneven surfaces. This is demonstrated in Fig. 3, which shows the area fraction of exposed hydroxyapatite after blasting under various conditions. A substantial area fraction of exposed hydroxyapatite

TABLE I Elastic properties assumed in the finite element analysis

Material	Young's modulus (GPa)	Poisson's ratio
Titanium alloy	100	0.3
Epoxy	1	0.3
Cortical bone	10	0.3
Plasma-sprayed hydroxyapatite	100	0.3

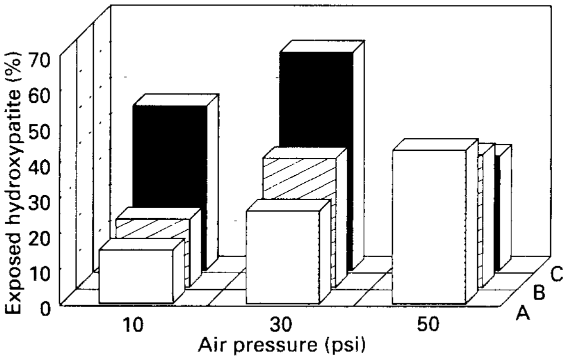

Figure 3 The area fraction of hydroxyapatite exposed after blasting under various conditions: (a) 10 s, at a shallow angle to the surface; (b) 10 s, normal to the surface and (c) 1 min, normal to the surface.

is produced over the whole range of blasting conditions, except at the shortest time and lowest air pressure. Fig. 4 shows an optical macrograph of a typical bead-blasted surface; the light areas indicate the considerable areas of exposed hydroxyapatite.

After blasting, sample coatings were etched to simulate resorption of the hydroxyapatite and examined in the SEM. Fig. 5 shows a normal view of the resulting surface; there are many hemispherical pores of 150–250 μm diameter, a size suitable for bone ingrowth.

Fig. 6 shows the edge of a typical particle in the coating during straining. At 0.5% strain there is no evidence of cracking; as the coating is strained further cracks appear at the edges of the particles and propagate around them.

The strength of bonding of the coatings to the substrate was assessed using a simple measurement of the critical strain energy release rate G_c. It was found that the strength of bonding of the adhesively bonded coating exceeded that of the cyanoacrylate adhesive used to bond the specimens (120 J m^{-2}). On the other hand, it was found that the plasma-sprayed coatings were weaker than the slight traces of adhesive which overlapped the edge of the specimens, and were therefore weaker than 1 J m^{-2} (bead blasted substrate) and 4 J m^{-2} (grit-blasted substrate).

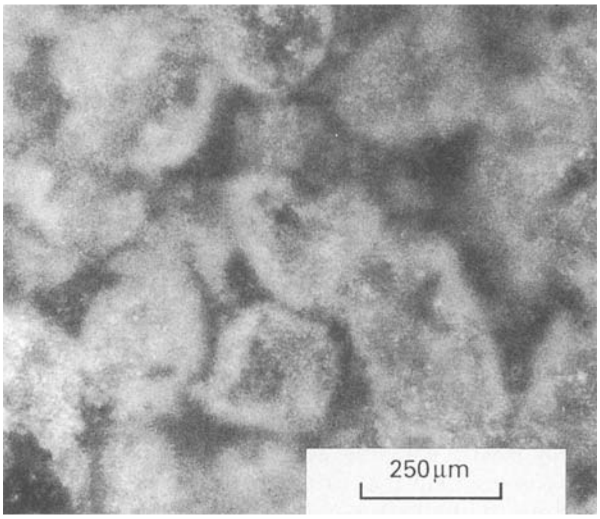

Figure 4 Optical macrograph showing a normal view of the surface of a typical blasted coating after staining with alizarin red S. The light areas are regions of exposed hydroxyapatite.

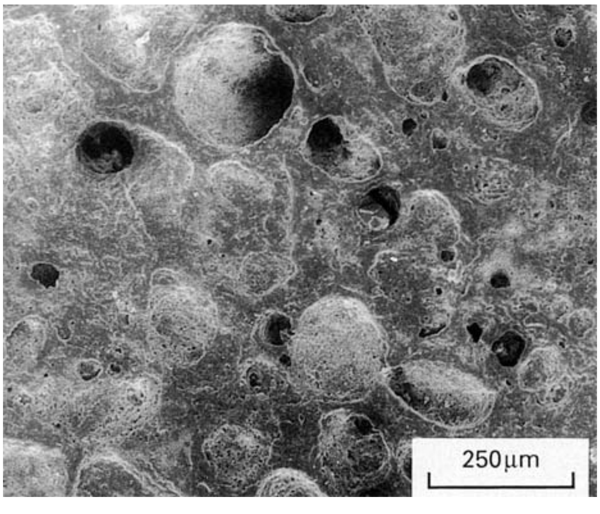

Figure 5 Scanning electron micrograph showing the surface of a bead-blasted coating after etching to simulate the resorption of the hydroxyapatite particles. The sites of the particles are visible as circular pits in the surface.

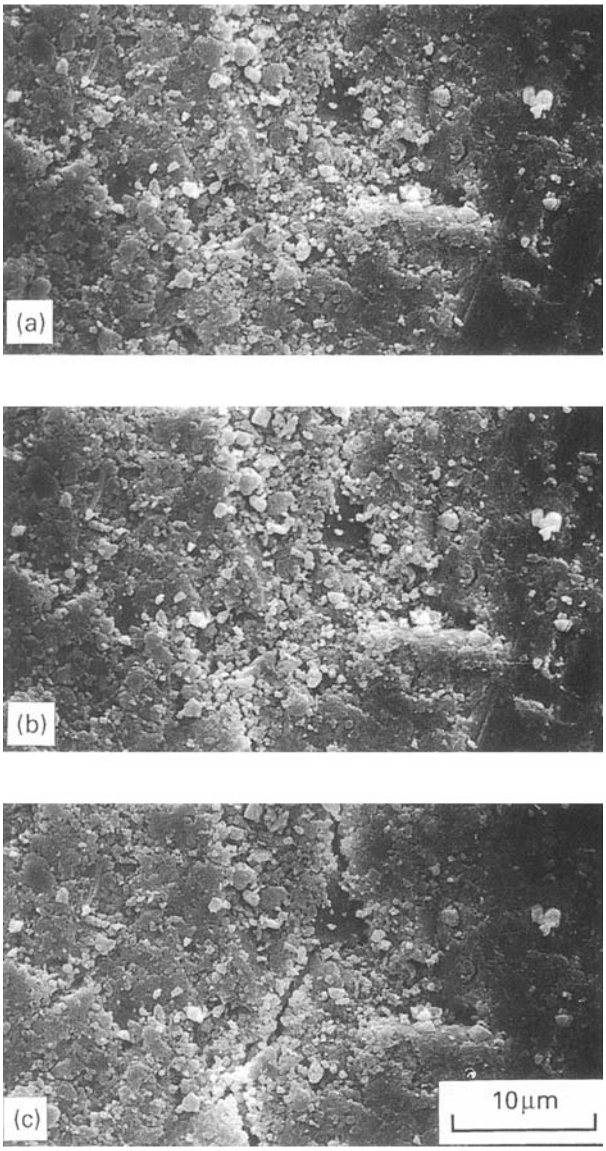

Figure 6 Scanning electron micrographs of the edge of a typical particle at strains of (a) 0.5%, (b) 1% and (c) 1.6% showing the formation and propagation of cracks.

Fig. 7 shows part of the results of the X-ray diffraction measurements in schematic form. In the case of the plasma-sprayed coating, there are small extra peaks at 29.5 and 31° 2θ which indicate the presence of α- and β-whitlockite. The peaks are also broadened in this coating as a result of the smaller crystallite size and possibly also residual thermal strains in the coating. In the case of the adhesively bonded coating, the extra peaks are absent indicating that the hydroxyapatite is pure and the peaks are narrower, indicating that the coating is more crystalline.

Fig. 8 shows the stress distribution in the bone around the tips of prostheses with the present adhesively bonded coating and a plasma-sprayed hydroxyapatite coating, together with the stress distribution in

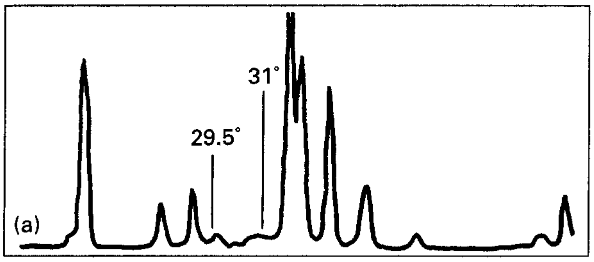

Plasma sprayed coating

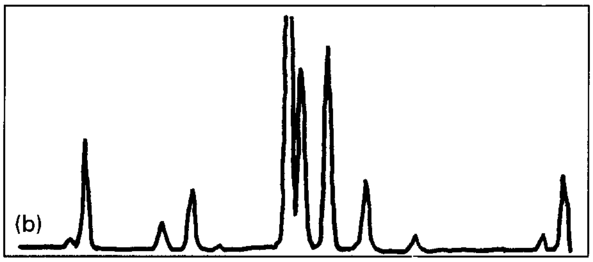

Adhesively bonded coating

Figure 7 Schematic X-ray diffraction results for (a) adhesively bonded and (b) plasma-sprayed coatings.

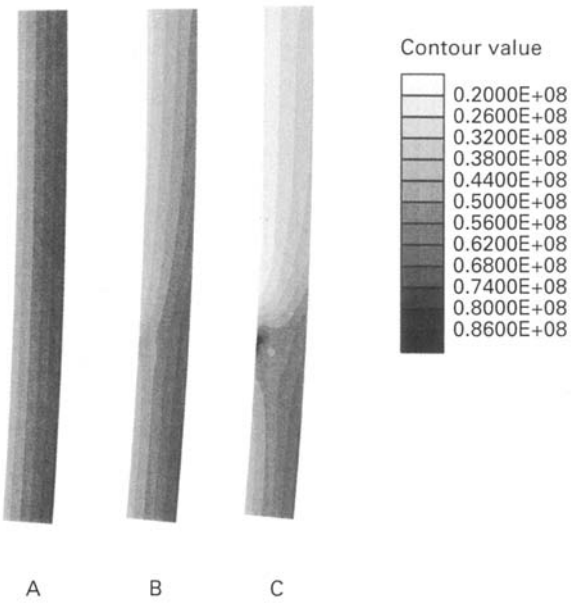

Figure 8 Von Mises stresses in the proximal part of the femoral diaphysis for (a) the natural femur, (b) the present coatings and (c) a plasma-sprayed hydroxyapatite coating.

the natural femur under the same loading for comparison. The contours show the Von Mises stress, as defined in Equation 1.

$$\sigma_v = (\sigma_x^2 + \sigma_y^2 + \sigma_z^2 - \sigma_x\sigma_y - \sigma_y\sigma_z - \sigma_x\sigma_z + 3\sigma_{xy}^2 + 3\sigma_{yz}^2 + 3\sigma_{xz}^2)^{1/2} \qquad (1)$$

Fig. 9 shows the shear stress along the implant–bone interface at the lateral edge of the distal tip of the prosthesis. In the case of the plasma-sprayed coating, there is a large stress concentration at the tip; this is relieved by the present layered coating.

4. Discussion

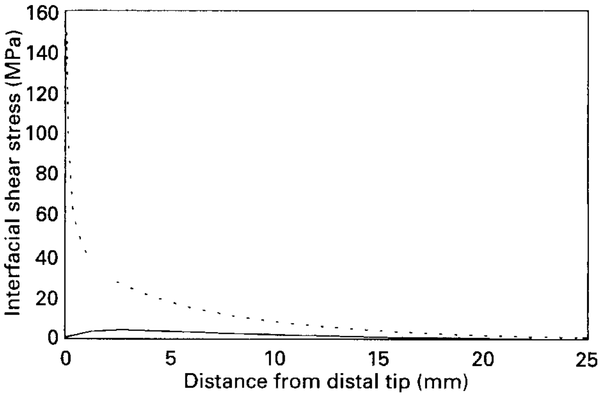

Figure 9 Interfacial shear stresses along the lateral edge of the prostheses, near the distal tip (——— 1 mm coating, ---- uncoated).

Adhesively bonded hydroxyapatite coatings offer a number of potential advantages over conventional plasma-sprayed coatings. Fatigue tests [6] have shown that plasma-sprayed coatings may have a detrimental effect on the fatigue strength of Ti–6Al–4V substrates, while adhesively bonded coatings have no such effect. The strain-to-failure tests show no evidence of damage until 1% strain, which compares favourably with the yield strain of Ti–6Al–4V (≈ 0.9%), whereas conventional plasma-sprayed coatings are severely damaged by residual thermal stresses before the substrate is strained at all. The critical strain energy release rate for debonding of the coatings from the substrate was found to be at least a hundred times that of a plasma-sprayed coating on a similar substrate and at least fifty times that of a plasma-sprayed coating on a grit-blasted substrate. The X-ray diffraction measurements presented here indicate that the adhesive bonding process avoids the formation of α- and β-whitlockite which can occur during plasma spraying, and results in a more crystalline coating than that produced by plasma spraying. Etching of the hydroxyapatite to simulate possible resorption *in vivo* showed the formation of hemispherical pores typically around 150 μm in diameter, which are appropriate for the ingrowth of bone to promote good fixation of the implant in the long term.

In the presence of an adhesively bonded coating, the stress concentrations that arise at the ends of the prosthesis are greatly reduced and there is a much more natural stress distribution in the bone around the prosthesis (Fig. 8). Similarly, Fig. 9 shows the reduction in interfacial stresses that can be obtained by the use of such coatings; the coatings cushion the implant and extend the regions of load transfer over a greater area of the implant–bone interface, thereby reducing the interfacial stresses. The authors have shown [7] that in the absence of some form of flexible interlayer very large stress concentrations may develop at the ends of the prosthesis which may preclude stable long-term fixation. A further study by the authors [8] has shown that the use of a structure with stiffness characteristics tailored to give optimum load transfer to the femur enables the control of the magnitude and direction of the interfacial stresses and enables a further large reduction in stress shielding.

An adhesively bonded hydroxyapatite coating with a flexible interlayer thus offers a number of potential advantages over conventional plasma-sprayed coatings. A method of applying such coatings has been described which permits their application to curved or textured surfaces; the resulting coatings have a substantial area of exposed hydroxyapatite ($\geq 30\%$) at the surface, the resorption of which creates pores of a suitable size and shape for bone ingrowth. The use of moulding or other techniques to produce a thicker interlayer could enable the construction of a prosthesis with any controlled stiffness characteristics, enabling the optimization of the pattern of load transfer and hence enhancing the mechanical compatibility of the prosthesis.

There are a number of possibilities for the use of such coatings in the design of novel prostheses with improved mechanical and biological compatibility. Thin adhesively bonded coatings offer a number of advantages as a direct replacement for conventional plasma sprayed hydroxyapatite coatings, subject to appropriate clinical trials. The use of coatings with thicker interlayers could lead to a substantial enhancement in the mechanical compatibility of existing cementless prostheses, through improvements in the pattern of load transfer and the relief of interfacial stress concentrations. Finally, there are possibilities for the development of novel implant designs incorporating layered structures of the type described here, enabling the optimization of load transfer from the prosthesis to the bone and hence offering much improved long-term stability.

5. Conclusions

A process has been developed which enables the production of layered, adhesively bonded hydroxyapatite coatings for orthopaedic implants. The coatings have a substantial area of exposed hydroxyapatite at the surface, and resorption of the hydroxyapatite leaves pores suitable for bone ingrowth. The coatings have a number of advantages over conventional plasma-sprayed hydroxyapatite coatings, including improved mechanical compatibility with the surrounding bone. The use of a layered structure with appropriate elastic properties can result in enhanced load transfer from the prosthesis to the bone, and permits the development of novel implant designs offering near-optimal load transfer to the bone and hence greatly improved long-term stability.

Acknowledgements

This work is funded by a CASE award from the Science and Engineering Research Council. The material and technical assistance of Mr M. Tuke (Finsbury (Instruments) Ltd, Chessington, Surrey) and Mr T. Baldwin (Permabond, Eastleigh, Hants) is gratefully acknowledged, as is the assistance of Dr P. Holdway (Defence Research Agency, Farnborough, Hants) who carried out the X-ray diffraction measurements.

References

1. P. O. KROON and M A. FREEMAN, *J. Bone Joint Surg* **74B** (1992) 518.
2. S D. COOK, K A. THOMAS, J. F. KAY and M JARCHO *Clin. Orthop.* **232** (1988) 225.
3. D. P. RIVERO, J. FOX, A. K. SKIPOR, R. M. URBAN and J. O. GALANTE, *J. Biomed. Mater. Res.* **22** (1988) 191.
4. C. P. A. T. KLEIN, P PATKA, H. B. M VAN DER LUBBE, J G. C. WOLKE and K DE GROOT, *J. Biomed. Mater. Res.* **25** (1991) 53.
5. S. L. EVANS and P J GREGSON, British Patent Application 93 00 746.6, January 1993.
6. S. L. EVANS and P. J. GREGSON, *Mater. Lett.* **16** (1993) 270.
7. S. L. EVANS and P. J. GREGSON, *J. Biomech.* (submitted) May 1993.
8. S L EVANS, and P. J. GREGSON, *J. Mater Sci.: Mater. Med.* (*in* press).